

Exchange Coupling and Magnetic Blocking in Bipyrimidyl Radical-Bridged Dilanthanide Complexes

Selvan Demir, Joseph M. Zadrozny, Michael Nippe, and Jeffrey R. Long*

Department of Chemistry, University of California, Berkeley, California 94720, United States

S Supporting Information

ABSTRACT: The synthesis and magnetic properties of three new bipyrimidyl radical-bridged dilanthanide complexes, $[(\text{Cp}^*_2\text{Ln})_2(\mu\text{-bpym}^\bullet)]^+$ (Ln = Gd, Tb, Dy), are reported. Strong $\text{Ln}^{\text{III}}\text{-bpym}^{\bullet-}$ exchange coupling is observed for all species, as indicated by the increases in $\chi_M T$ at low temperatures. For the Gd^{III} -containing complex, a fit to the data reveals antiferromagnetic coupling with $J = -10 \text{ cm}^{-1}$ to give an $S = 13/2$ ground state. The Tb^{III} and Dy^{III} congeners show single-molecule magnet behavior with relaxation barriers of $U_{\text{eff}} = 44(2)$ and $87.8(3) \text{ cm}^{-1}$, respectively, a consequence of the large magnetic anisotropies imparted by these ions. Significantly, the latter complex exhibits a divergence of the field-cooled and zero-field-cooled dc susceptibility data at 6.5 K and magnetic hysteresis below this temperature.

Single-molecule magnets are molecules that possess an energy barrier to spin inversion, leading to slow magnet relaxation and, in the absence of rapid tunneling, magnetic hysteresis at low temperatures. For example, the original single-molecule magnet, $\text{Mn}_{12}\text{O}_{12}(\text{O}_2\text{CMe})_{16}(\text{H}_2\text{O})_4$, displays an exchange-coupled $S = 10$ ground state with an effective spin reversal barrier of $U_{\text{eff}} = 42 \text{ cm}^{-1}$, leading to a magnetic relaxation time of 2 months at 2 K and, consequently, magnetic hysteresis.¹ For proposed applications, such as high-density information storage, quantum computing, or spintronics, it is essential, however, to develop molecules exhibiting this type of behavior at significantly higher temperatures.²

Recent developments in the field have demonstrated that much larger spin reversal barriers are accessible in lanthanide-containing complexes,³ on account of the large single-ion magnetic anisotropy delivered by an appropriate configuration of 4f electrons.⁴ Unfortunately, in the absence of substantial magnetic exchange coupling, these species tend to display relaxation *via* tunneling pathways that shortcut the thermal relaxation barrier and eliminate the remnant magnetization in a typical hysteresis measurement. In contrast, the N_2^{3-} radical-bridged dilanthanide complexes $\{[(\text{Me}_3\text{Si})_2\text{N})_2\text{Ln}(\text{THF})_2(\mu\text{-}\eta^2\text{:}\eta^2\text{-N}_2)]\}^-$ (Ln = Gd, Tb, Dy, Ho, Er) in some cases display unusually long relaxation times at low temperatures, owing to the rare combination of large lanthanide ion magnetic anisotropy and strong exchange coupling.⁵ Indeed, the Tb^{III} congener exhibits hysteresis up to a record magnetic blocking temperature for a molecular species of 14 K.^{5b} Although the diffuse spin orbital of the N_2^{3-} bridge is evidently suitable for creating a strong direct exchange with unpaired electrons in the

contracted 4f orbitals of the lanthanide ions,⁶ employing this highly reactive unit for the controlled synthesis of larger molecular clusters is extremely challenging. Furthermore, the N_2^{3-} ligand is not viable for simple synthetic modification to tune the magnetic exchange coupling. We therefore chose to explore the possibility of instead employing more controllable organic radical bridging ligands to achieve a similar effect. Recognizing its well-established bridge-forming capabilities,⁷ together with its reversible electrochemical reduction at -1.73 V versus SCE in DMF,⁸ we decided to pursue reduced dilanthanide complexes of 2,2'-bipyrimidine (bpym). Herein, we describe the synthesis, structural characterization, and magnetic properties of salts of three new dilanthanide complexes, $[(\text{Cp}^*_2\text{Ln})_2(\mu\text{-bpym}^\bullet)]$ (BPh_4) (Cp* = pentamethylcyclopentadienyl; Ln = Gd (1), Tb (2), Dy (3)), the first such species in which the bridging ligand is the radical anion $\text{bpym}^{\bullet-}$.

Compounds 1–3 were synthesized by mixing $\text{Cp}^*_2\text{Ln}(\text{BPh}_4)$ (Ln = Gd, Tb, Dy)⁹ and bpym together in THF and subsequent reduction with potassium graphite (Figure 1). Layering of THF solutions of the products with Et_2O at $-35 \text{ }^\circ\text{C}$ afforded crystals suitable for X-ray analysis.¹⁰ All three compounds are isostructural, each featuring a dilanthanide complex that resides on a crystallographic inversion center, such that the two metal

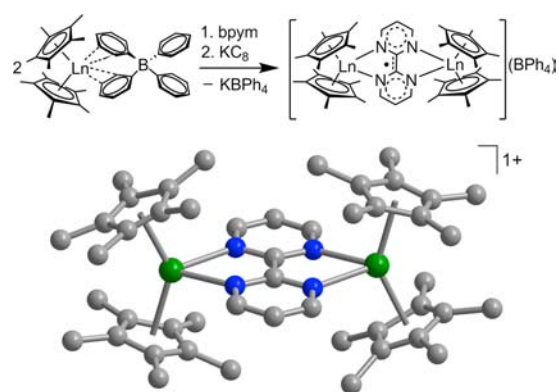


Figure 1. Upper: Synthetic scheme for 1 (Ln = Gd), 2 (Ln = Tb), and 3 (Ln = Dy). Lower: Structure of the bipyrimidyl radical-bridged cation in a crystal of 3. Green, blue, and gray spheres represent Dy, N, and C atoms, respectively; H atoms are omitted for clarity. 1 and 2 are isostructural. Selected interatomic distances (Å) for 2 and 3, respectively: C(2)–C(2') 1.396(9), 1.401(3); mean Ln–N(bpym[•]) 2.44(1), 2.42(1); Ln...Ln 6.460(1), 6.425(1).

Received: September 8, 2012

Published: October 30, 2012

centers are equivalent by symmetry (Figures 1, S1 and S2, Supporting Information). Each metal is coordinated by two Cp* ligands and two N atoms of a bridging bpym^{•−} ligand. Consistent with the radical character of the bridge, the central C(2)–C(2′) bond distances are 1.396(9) Å for **2** and 1.401(3) Å for **3**, significantly shorter than the mean value of 1.48(2) Å found for dilanthanide complexes bridged by neutral bpym and 1.501(1) Å for free 2,2′-bipyrimidine.¹¹ Importantly, based upon the LUMO calculated for a neutral bpym ligand,⁸ the radical spin orbital of bpym^{•−} is expected to have not only the largest contributions from in-phase 2p_z orbitals on the central two C atoms but also substantial contributions of opposite phase from the 2p_z orbitals on the surrounding four N atoms.

Dc magnetic susceptibility data were collected on samples of **1–3** at 2–300 K to probe for the possible presence of magnetic exchange coupling (Figure 2). For all compounds, the values of

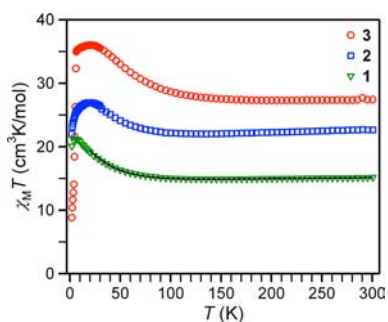


Figure 2. Variable-temperature dc magnetic susceptibility data for restrained polycrystalline samples of **1–3** collected under a 1 kOe applied dc field. The black line represents a fit to the data for **1**, as discussed in the main text.

$\chi_M T$ at rt (15.14, 22.65, and 27.40 cm³K/mol for **1–3**, respectively) are slightly lower than that expected for two noninteracting lanthanide ions and a radical spin center (16.13, 24.00, and 28.71 cm³K/mol, respectively). As the temperature is lowered, a slight decrease in $\chi_M T$ is apparent, reaching a shallow minimum at 135, 135, and 200 K for **1–3**, respectively (Figure S3). This is followed by a rise in $\chi_M T$, suggestive of a high-angular momentum ground state obtained as a result of antiferromagnetic coupling between the radical bridging ligand and the lanthanide ions. At even lower temperatures, $\chi_M T$ decreases again, gradually for **1** and **2** but precipitously for **3**. The nearly discontinuous drop in $\chi_M T$ for **3** at <7 K is one indication of magnetic blocking, as was previously observed for N₂^{3−} radical-bridged Tb^{III} and Dy^{III} complexes.⁵ Consistently, field- and zero-field-cooled magnetic susceptibility data collected for **3** show a sharp divergence at 6.5 K (Figure S4).

For most lanthanide compounds, a precise determination of the strength and sign of the exchange coupling constant (J) is complicated by the intricate electronic structures of the individual lanthanide ions. In contrast, the metal centers in Gd^{III} compounds possess a 4f⁷ electron configuration with $S = 7/2$, making them suitable for analyzing magnetic exchange coupling, due to spin-only behavior free of complications from spin–orbit coupling. Accordingly, the $\chi_M T$ data for **1** were fit to the spin-only Hamiltonian $\hat{H} = -2J\hat{S}_{\text{rad}}(\hat{S}_{\text{Gd}(1)} + \hat{S}_{\text{Gd}(2)})$, where J represents intramolecular Gd^{III}–radical exchange coupling and \hat{S}_i are the spin operators for each paramagnetic center. Variable-field, variable-temperature magnetic susceptibility data for **1** (Figure S5) indicate that the slight downturn in $\chi_M T$ at very low temperature is due to the Zeeman effect. Since the impact of this

is significant only below 20 K, only data collected above that temperature were included in the fitting procedure. The best fit afforded $J = -10 \text{ cm}^{-1}$ (Figure 2), indicating antiferromagnetic Gd^{III}–radical coupling to give an $S = 13/2$ ground state. To our knowledge, this J value is the second largest in magnitude yet reported for a Gd^{III} compound, only surpassed by the $J = -27 \text{ cm}^{-1}$ observed for the N₂^{3−} radical-bridged complex $\{[(\text{Me}_3\text{Si})_2\text{N}]_2\text{Gd}(\text{THF})_2(\mu-\eta^2:\eta^2-\text{N}_2)\}^{-5a,12}$.

The similar trends observed in the temperature dependence of the $\chi_M T$ data for **2** and **3** indicate that they too possess a strong antiferromagnetic coupling between the Ln^{III} centers and the radical bridging ligand. Indeed, the temperatures at which the shallow minima in the data occur suggest that $|J(1)| \approx |J(2)| < |J(3)|$. This ordering is somewhat unexpected, since, with a slightly smaller ionic radius, Dy^{III} would generally have more contracted valence orbitals than Gd^{III} or Tb^{III}. Similar considerations for the N₂^{3−} radical-bridged dilanthanide complexes suggest that the strength of the exchange interactions follows the opposite trend: Tb^{III} > Dy^{III} > Ho^{III} > Er^{III}.⁵ Overall, the results suggest that perhaps the exchange coupling in **1–3** is via a spin-polarization mechanism involving the empty Ln^{III} 5d orbitals, rather than direct exchange interactions between the radical spin orbital and the Ln^{III} 4f orbitals.

In view of the large magnetic anisotropy associated with Tb^{III} and Dy^{III}, it was anticipated that **2** and **3** would exhibit slow magnetic relaxation. Ac magnetic susceptibility data collected for these compounds indeed display out-of-phase susceptibility (χ_M'') signals with a frequency and temperature dependence indicative of long magnetic relaxation times. From 2 to 3 K, under ac frequencies ranging from 1 to 1500 Hz, **2** shows a peak maximum at 47 Hz in χ_M'' that decreases in intensity with increasing temperature, but remains invariant with respect to frequency (Figure S6). The peak begins to shift to higher frequencies at temperatures above 3 K, ultimately moving beyond the frequency limit of the magnetometer at 7.5 K. In contrast, as shown in Figure 3, when **3** was subjected to an ac magnetic field of 0.1–1500 Hz at temperatures 7.5–17.5 K, the χ_M'' peak maximum changed frequency over the entire temperature range probed. Quantitative determination of magnetic relaxation times (τ) for **2** and **3** as a function of temperature was performed via the construction of Cole–Cole plots for each temperature (Figures S7 and S8) and subsequent fitting of the plots to a generalized Debye model.

The temperature dependence of τ can provide useful information about the operative magnetic relaxation processes at particular temperatures for a given system. In particular, in the presence of an activation barrier with respect to moment reversal, the system must exchange energy with the lattice (in the form of phonons) to ascend to the top of the barrier before relaxation can occur. Such a relaxation mechanism, known as an Orbach process,¹³ leads to an exponential dependence of τ upon temperature. Thus, one can generate an Arrhenius plot to determine the energy barrier U_{eff} and attempt time τ_0 , as shown in Figure 4 for **2** and **3**.

For **2**, at 2–3 K, τ is temperature-independent, which indicates that magnetic relaxation does not require the input or release of energy to the lattice. This phenomenon is usually observed for relaxation processes where the moment tunnels through the relaxation barrier. At temperatures above 3 K, however, τ becomes temperature-dependent, suggesting an approach to Arrhenius behavior and an Orbach relaxation mechanism. A linear fit to the relaxation times observed between 6 and 7 K affords an effective spin reversal barrier of $U_{\text{eff}} = 44(2) \text{ cm}^{-1}$ and

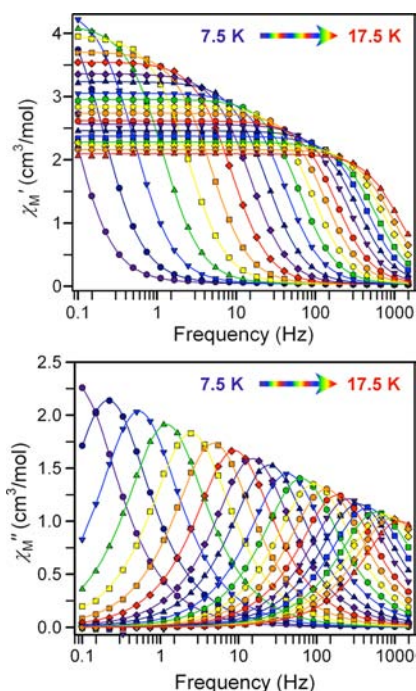


Figure 3. In-phase (χ_M' , top) and out-of-phase (χ_M'' , bottom) components of the ac magnetic susceptibility for **3** under zero applied dc field from 7.5 K (purple circles) to 17.5 K (red triangles). Solid lines represent fits to the data, as described in the main text.

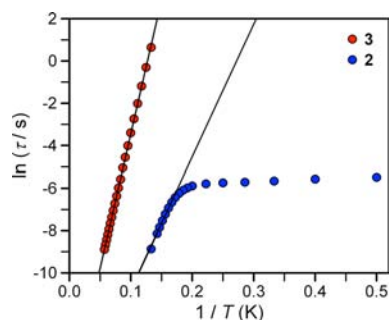


Figure 4. Arrhenius plots of relaxation time data for **2** and **3**. The black lines correspond to linear fits to the Arrhenius equation, as described in the main text, yielding $U_{\text{eff}} = 44(2) \text{ cm}^{-1}$ and $\tau_0 = 4(1) \times 10^{-8} \text{ s}$ for **2** and $U_{\text{eff}} = 87.8(3) \text{ cm}^{-1}$ and $\tau_0 = 1.03(4) \times 10^{-7} \text{ s}$ for **3**.

an attempt time of $\tau_0 = 4(1) \times 10^{-8} \text{ s}$. The value for the barrier is higher than the range normally observed for single-molecule magnets, and **2** can be placed among a small but growing set of Tb^{III}-based single-molecule magnets.¹⁴ In contrast, the τ values for **3** are fully temperature dependent, indicating that an Orbach process is operative over the entire temperature and frequency range investigated. A fit to the Arrhenius expression affords a much higher relaxation barrier of $U_{\text{eff}} = 87.8(3) \text{ cm}^{-1}$, with $\tau_0 = 1.03(4) \times 10^{-7} \text{ s}$. Significantly, this eclipses the value of $U_{\text{eff}} = 67 \text{ cm}^{-1}$ reported for a dinuclear Co^{II} carbene radical-bridged complex,¹⁵ which is the largest barrier known for an exchange-coupled transition metal species. It should be noted that the values of τ_0 for **2** and **3** are within the expected range for single-molecule magnets.

Although large, the relaxation barriers for **2** and **3** fall short of those observed for perhaps a dozen other molecules.^{3k,4} The N₂³⁻ radical-bridged complexes, which represent the most closely related species, display relaxation barriers of 227 and

123 cm⁻¹ for Tb^{III} and Dy^{III}, respectively, possibly as a result of the stronger exchange coupling. For comparison, the largest barriers yet reported for mono- and multinuclear species are 566 cm⁻¹ for the phthalocyanine sandwich complex Tb^{III}Pc₂^{14h} and 367 cm⁻¹ for the square pyramidal cluster Dy₅O(OⁱPr)₁₃.^{3k} In cluster complexes such as the latter species, the single-molecule magnet behavior is thought to originate largely from the strong anisotropy of the Dy^{III} centers, with only weak contributions from intramolecular exchange coupling. This can lead to multinuclear complexes that display magnetization dynamics corresponding to multiple slowly relaxing Dy^{III} centers, rather than from a fully exchange-coupled moment.^{3b,d} Furthermore, regardless of the thermal relaxation barrier obtained from ac susceptibility measurements, which can be very high, the fact that the slow magnetic relaxation stems largely from the moments of individual ions allows for the occurrence of faster, tunneling relaxation processes that shortcut the barrier. While the origins of these processes are not necessarily fully understood for lanthanide-based systems, some studies have suggested that intermolecular dipolar interactions are important.¹⁶

The ultimate test for the utility of a single-molecule magnet lies in the evaluation of its magnetic hysteresis behavior. At 2 K and below, under an average sweep rate of 0.003 T/s, **2** displays a waist-constricted hysteresis loop that is closed at zero field and slightly opens at higher fields (Figure S9). This result is consistent with the relaxation times obtained from the ac susceptibility measurements and the presence of tunneling at zero applied dc field. In contrast, the hysteresis loops collected for a polycrystalline sample of **3** are open at zero field for temperatures up to 6.5 K (Figure 5). The coercive field retains its

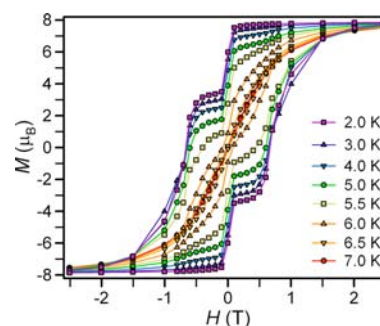


Figure 5. Variable-field magnetization (M) data for compound **3** collected from 2 to 7 K at an average sweep rate of 0.002 T/s.

maximum of $H_c = 0.6 \text{ T}$ up to 3 K but then steadily decreases as the temperature is raised. Note that the presence of a prominent step in the hysteresis loop at $H = 0$ indicates that tunneling, which was not apparent on the much faster time scale probed by the ac susceptibility measurements, is indeed occurring in this sample. Significantly, however, only four molecules have been shown to have a higher maximum temperature for magnetic hysteresis when measured under similar field sweep rates: 7 K for Dy₄(OH)₂(bmh)₂(msh)₄Cl₂,^{3b} 7 K for Tb^{III}Pc₂^{14h} and 8.3 and 14 K for the N₂³⁻ radical-bridged complexes of Dy^{III} and Tb^{III}, respectively.⁵

Interestingly, the U_{eff} values and the magnetic hysteresis data indicate that the Dy^{III} compound **3** is a better single-molecule magnet than its Tb^{III} analogue **2**. This is in contrast to the observations for the N₂³⁻ radical-bridged complexes and counters the expectation that Tb^{III} centers should deliver a greater magnetic anisotropy.⁴ We speculate that the difference

stems from the weaker magnetic exchange coupling apparent for **2**, consistent with the idea that the relaxation barrier for such molecules is related to the amount of energy needed to overwhelm their tendency to behave as a large collective magnetic moment (i.e., the giant spin model).^{12b} This, with the lack of tunneling apparent for the more strongly coupled N_2^{3-} radical-bridged species,⁵ suggests the need to enhance the strength of the exchange coupling in organic radical-bridged lanthanide systems. We also note that the specific coordination environments of the Ln^{III} centers in such complexes are also likely to have a significant influence on the relaxation barrier and tunneling probability and provide another important variable for future study via terminal ligand modification.

The foregoing results demonstrate that strong magnetic coupling and single-molecule magnet behavior, including magnetic blocking, can be achieved in bipyrimidyl radical-bridged dilanthanide complexes. In particular, the large degree of tunability that can be envisioned for such systems is of importance. Efforts are now underway, for example, to generate higher-nuclearity $bpym^{\bullet-}$ -bridged species with larger ground state moments, as well as to increase the strength of the magnetic exchange coupling through addition of electron-donating or -withdrawing substituents to the $bpym$ ligand. In addition, the many various other organic radical bridging ligands that would place a high spin density on the donor atoms coordinating to a lanthanide ion are clearly in need of exploration.

■ ASSOCIATED CONTENT

Supporting Information

Full experimental details, crystallographic, and additional magnetic data. This material is available free of charge via the Internet at <http://pubs.acs.org>.

■ AUTHOR INFORMATION

Corresponding Author

jrlong@berkeley.edu

Notes

The authors declare no competing financial interest.

■ ACKNOWLEDGMENTS

This work was funded by NSF Grant No. CHE-1111900. We thank the Postdoctoral Program of the German Academic Exchange Service (DAAD) for fellowship support of S.D. and Tyco Electronics for fellowship support of J.M.Z.

■ REFERENCES

- (1) (a) Sessoli, R.; Tsai, H. L.; Schake, A. R.; Wang, S.; Vincent, J. B.; Folting, K.; Gatteschi, D.; Christou, G.; Hendrickson, D. N. *J. Am. Chem. Soc.* **1993**, *115*, 1804. (b) Sessoli, R.; Gatteschi, D.; Caneschi, A.; Novak, M. A. *Nature* **1993**, *365*, 141.
- (2) (a) Leuenberger, M. N.; Loss, D. *Nature* **2001**, *410*, 789. (b) Ardavan, A.; Rival, O.; Morton, J. J. L.; Blundell, S. J.; Tyryshkin, A. M.; Timco, G. A.; Winpenny, R. E. P. *Phys. Rev. Lett.* **2007**, *98*, 057201–1. (c) Bogani, L.; Wernsdorfer, W. *Nat. Mater.* **2008**, *7*, 179. (d) Stamp, P. C. E.; Gaita-Ariño, A. J. *Mater. Chem.* **2009**, *19*, 1718. (e) Luis, F.; Repollés, A.; Martínez-Pérez, M. J.; Aguilà, D.; Roubeau, O.; Zueco, D.; Alonso, P. J.; Evangelisti, M.; Camón, A.; Sesé, J.; Barrios, L. A.; Aromí, G. *Phys. Rev. Lett.* **2011**, *107*, 117203.
- (3) (a) Ishikawa, N.; Mizuno, Y.; Takamatsu, S.; Ishikawa, T.; Koshihara, S.-y. *Inorg. Chem.* **2008**, *47*, 10217. (b) Lin, P.-H.; Burchell, T. J.; Unger, L.; Chibotaru, L. F.; Wernsdorfer, W.; Murugesu, M. *Angew. Chem., Int. Ed.* **2009**, *48*, 9489. (c) AlDamen, M. A.; Cardona-Serra, S.; Clemente-Juan, J. M.; Coronado, E.; Gaita-Ariño, A.; Martí-Gastaldo, C.; Luis, F.; Montero, O. *Inorg. Chem.* **2009**, *48*, 3467. (d) Guo, Y.-N.;

- Xu, G.-F.; Gamez, P.; Zhao, L.; Lin, S.-Y.; Deng, R.; Tang, J.; Zhang, H.-J. *J. Am. Chem. Soc.* **2010**, *132*, 8538. (e) Hewitt, I. J.; Tang, J.; Madhu, N. T.; Anson, C. E.; Lan, Y.; Luzon, J.; Etienne, M.; Sessoli, R.; Powell, A. K. *Angew. Chem., Int. Ed.* **2010**, *49*, 6352. (f) Layfield, R. A.; McDouall, J. J. W.; Sulway, S. A.; Tuna, F.; Collison, D.; Winpenny, R. E. P. *Chem.—Eur. J.* **2010**, *16*, 4442. (g) Jiang, S.-D.; Wang, B.-W.; Sun, H.-L.; Wang, Z.-M.; Gao, S. *J. Am. Chem. Soc.* **2011**, *133*, 4730. (h) Long, J.; Habib, F.; Lin, P.-H.; Korobkov, I.; Enright, G.; Ungur, L.; Wernsdorfer, W.; Chibotaru, L. F.; Murugesu, M. *J. Am. Chem. Soc.* **2011**, *133*, 5319. (i) Watanabe, A.; Yamashita, A.; Nakano, M.; Yamamura, T.; Kajiwara, T. *Chem.—Eur. J.* **2011**, *17*, 7428. (j) Feltham, H. L. C.; Clérac, R.; Powell, A. K.; Brooker, S. *Inorg. Chem.* **2011**, *50*, 4232. (k) Blagg, R. J.; Muryn, C. A.; McInnes, E. J. L.; Tuna, F.; Winpenny, R. E. P. *Angew. Chem., Int. Ed.* **2011**, *50*, 6530.
- (4) Rinehart, J. D.; Long, J. R. *Chem. Sci.* **2011**, *2*, 2078.
 - (5) (a) Rinehart, J. D.; Fang, M.; Evans, W. J.; Long, J. R. *Nat. Chem.* **2011**, *3*, 538. (b) Rinehart, J. D.; Fang, M.; Evans, W. J.; Long, J. R. *J. Am. Chem. Soc.* **2011**, *133*, 14236.
 - (6) Rajeshkumar, T.; Rajaraman, G. *Chem. Commun.* **2012**, *48*, 7856.
 - (7) De Munno, G.; Lloret, F.; Julve, M. In *Magnetism: A Supramolecular Function*; Kahn, O., Ed.; Kluwer: Dordrecht, The Netherlands, 1996; p 555 and references therein.
 - (8) Kaim, W.; Kohlmann, S. *Inorg. Chem.* **1987**, *26*, 68.
 - (9) The compounds $Cp^*_2Ln(BPh_4)$ ($Ln = Tb, Dy$) were synthesized in a manner similar to that previously reported for $Cp^*_2Gd(BPh_4)$: Evans, W. J.; Davis, B. L.; Champagne, T. M.; Ziller, J. W. *Proc. Natl. Acad. Sci. U.S.A.* **2006**, *103*, 12678.
 - (10) **1** is isostructural with **2** and **3**. While the molecular connectivity could be unambiguously determined, the poor quality of the best diffraction data obtained prohibits a more in-depth discussion of bond lengths and angles. Unit cell parameters: $a = 11.0434(8)$ Å, $b = 28.505(2)$ Å, $c = 24.221(2)$ Å, $\beta = 101.018(4)^\circ$, $V = 7484.0(10)$ Å³.
 - (11) (a) Berg, D. J.; Boncella, J. M.; Andersen, R. A. *Organometallics* **2002**, *21*, 4622. (b) Zucchi, G.; Jeon, T.; Tondelier, D.; Aldakov, D.; Thuéry, P.; Ephritikhine, M.; Geffroy, B. *J. Mater. Chem.* **2010**, *20*, 2114. (c) Visinescu, D.; Fabelo, O.; Ruiz-Pérez, C.; Lloret, F.; Julve, M. *CrystEngComm* **2010**, *12*, 2454.
 - (12) (a) The contracted 4f orbitals of Gd^{III} more typically permit only very weak magnetic exchange interactions, with $|J| \leq 3$ cm⁻¹: Benelli, C.; Gatteschi, D. *Chem. Rev.* **2002**, *102*, 2369. (b) The Hubbard model discussed here provides one means of understanding the exchange coupling in N_2^{3-} -bridged complexes: Lukens, W. W.; Magnani, N.; Booth, C. H. *Inorg. Chem.* **2012**, *51*, 10105.
 - (13) (a) Orbach, R. *Proc. R. Soc. London, Ser. A* **1961**, *264*, 458. (b) Orbach, R. *Proc. R. Soc. London, Ser. A* **1961**, *264*, 485.
 - (14) (a) Ishikawa, N.; Sugita, M.; Ishikawa, T.; Koshihara, S.-y.; Kaizu, Y. *J. Am. Chem. Soc.* **2003**, *125*, 8694. (b) Novitchi, G.; Costes, J.-P.; Tuchagues, J.-P.; Vendier, L.; Wernsdorfer, W. *New J. Chem.* **2008**, *32*, 197. (c) Costes, J.-P.; Shova, S.; Wernsdorfer, W. *Dalton Trans.* **2008**, 1843. (d) Kajiwara, T.; Takahashi, K.; Hiraizumi, T.; Takaishi, S.; Yamashita, M. *Polyhedron* **2009**, *28*, 1860. (e) Lopez, N.; Prosvirin, A. V.; Zhao, H.; Wernsdorfer, W.; Dunbar, K. R. *Chem.—Eur. J.* **2009**, *15*, 11390. (f) Gonidec, M.; Luis, F.; Vilchez, À.; Esquena, J.; Amabilino, D. B.; Veciana, J. *Angew. Chem., Int. Ed.* **2010**, *49*, 1623. (g) Long, J.; Chamoreau, L.-M.; Marvaud, V. *Dalton Trans.* **2010**, *39*, 2188. (h) Gonidec, M.; Biagi, R.; Corradini, V.; Moro, F.; De Renzi, V.; del Pennino, U.; Summa, D.; Muccioli, L.; Zannoni, C.; Amabilino, D. B.; Veciana, J. *J. Am. Chem. Soc.* **2011**, *133*, 6603.
 - (15) Yoshihara, D.; Karasawa, S.; Koga, N. *J. Am. Chem. Soc.* **2008**, *130*, 10460.
 - (16) (a) Ishikawa, N.; Sugita, M.; Ishikawa, T.; Koshihara, S.-y.; Kaizu, Y. *J. Phys. Chem. B* **2004**, *108*, 11265. (b) Jiang, S.-D.; Wang, B.-W.; Su, G.; Wang, Z.-M.; Gao, S. *Angew. Chem., Int. Ed.* **2010**, *49*, 7448. (c) Car, P.-E.; Perfetti, M.; Mannini, M.; Favre, A.; Caneschi, A.; Sessoli, R. *Chem. Commun.* **2011**, *47*, 3751. (d) Habib, F.; Lin, P.-H.; Long, J.; Korobkov, I.; Wernsdorfer, W.; Murugesu, M. *J. Am. Chem. Soc.* **2011**, *133*, 8830. (e) Meihaus, K. R.; Rinehart, J. D.; Long, J. R. *Inorg. Chem.* **2011**, *50*, 8484. (f) Jiang, S.-D.; Liu, S.-S.; Zhou, L.-N.; Wang, B.-W.; Wang, Z.-M.; Gao, S. *Inorg. Chem.* **2012**, *51*, 3079.